Enhancing the Coverage of Underwater Robot Based Mn-crust Survey Area by Using a Multibeam Sonar

Umesh Neettiyath[1], Mehul Sangekar[2,1], Kazunori Nagano[1], Tetsu Koike[1], Blair Thornton[3,1], Harumi Sugimatsu[1], Hikari Hino[4], Akiko Suzuki[4]

[1]Institute of Industrial Science, The University of Tokyo, Komaba, 153-8505, Japan
(E-mail: umesh@iis.u-tokyo.ac.jp)
[2]X-STAR, Japan Agency for Marine-Earth Science and Technology, Yokosuka, Japan
[3]Southampton Marine and Maritime Institute, University of Southampton, Southampton SO16 7QF, UK
[4]Japan Organization for Metals and Energy Security, Toranomon, 105-0001, Japan

Abstract—The authors conducted a field survey of Cobalt-rich Manganese Crusts (Mn-crusts) using a visual 3D mapping system and a multibeam sonar mounted on an underwater robot for studying the distribution of these resources on the seafloor. The multibeam sonar covers an area 4 times that of the visual system and generates bathymetric and backscatter information. This paper shows preliminary results from field trials, showing the correlations between the multibeam and visual mapping data in Mn-crust covered seamounts. Further, the possibility of characterization of the seafloor using multibeam data is investigated by classifying the multibeam data using transfer learning of a classifier trained on visual mapping data. It is advantageous because co-located visual data can be used as a ground truth for multibeam classification. Mn-crust volumetric estimation methods, currently limited to visually mapped regions, can be extended further using these results.

I. INTRODUCTION

Cobalt-rich manganese crusts (Mn-crust) are gaining popularity as a potential source of valuable minerals including Cobalt, Nickel, and rare earth elements. These are hydrogenetic deposits found mainly on the slopes and shoulders of seamounts ranging from 800m to 2400m [1]–[5]. In order to explore these resources, the International Seabed Authority has assigned exploration slots to several countries. One third of the exploration area will be eventually allotted for seabed mining of Mn-crusts [6].

In order to estimate the resource potential of these areas, several methods have been attempted and used by stakeholders. Most of these are based on core drills, for assessing the Mn-crust thickness and chemical composition. Towed camera or Remotely Operated Vehicles (ROV) surveys are used for visually inspecting and confirming the Mn-crust covered areas. Ship based multibeam data is used for large area resource estimation, when combined with either core samples, seafloor videos, image surveys or sub-bottom profiles [7]–[10]. Since none of these methods could provide a continuous thickness measurement, an acoustic sub-bottom probe for in-situ contactless thickness measurement was developed by the Institute of Industrial Science of the University of Tokyo [11].

By combining thickness measurements with a high resolution 3D color mapping system, volumetric estimations of Mn-crust were performed [12]. However, since thickness measurements require low attitude surveys, the swath of the visually observed area is limited to about 1.5m.

In order to cover larger areas, the authors attempted to use a multibeam sonar in conjunction with the thickness and visual mapping system. Since the multibeam sonar used has a swath of 120°, an area 4 times that of visual mapping systems can be covered, albeit at a lower resolution. In addition, multibeam backscatter information is useful for seafloor characterization [13], [14]. While there were attempts to quantify the distribution of Mn-nodules using multibeam surveys [15], [16] or side scan sonar surveys [17], [18], this is the first such attempt for Mn-crusts. Mn-crusts are distinguished from Mn-nodules by the highly varying terrain and the necessity to measure the crust thickness. Therefore, it provides a challenge for low-altitude surveying and creates multipath reflections interfering with the sonar data analysis.
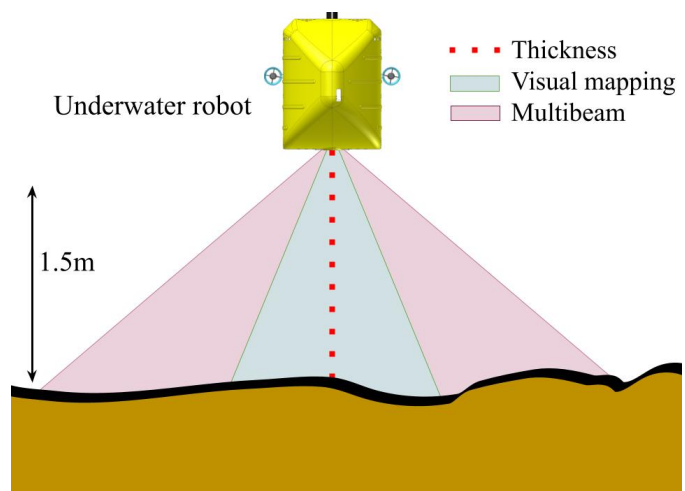

Fig. 1. Illustration of the mapping scenario

Delta-T Multibeam sonar	
Frequency	260 kHz
Transducer Beam Width	$120° \times 3°$
Number of beams	120
Beam resolution	$1°$
Horizontal opening angle	$120°$
Min. Range	0.5 m
Range resolution	0.02 % of range
Frame rate	15 fps
Visual mapping system	
Camera	1328×1048
Horizontal opening angle	$65°$
Vertical opening angle	$53°$
Laser to camera baseline	1.22 m
Frame rate	15 fps
Acoustic Probe	
Frequency	2 MHz (carrier), 200kHz (signal)
-3 dB footprint	< 2 cm (dynamic focusing)
Ping rate	20 Hz

Rest of this paper is organized as follows. A description of the systems used in the survey are described in section II. Section III details the field survey, the data processing methods and preliminary results from selected areas. Section IV investigates the possibility of applying a machine learning system on the multibeam data to estimate the Mn-crust coverage, using visual data as a reference. Section V contains the concluding remarks and future directions.

II. SYSTEM OVERVIEW

The different systems which are used in this work are described in this section. The three systems used consist of a wide swath multibeam sonar, a narrow swath visual mapping system and a point measurement sub-bottom probe. They are operated from an ROV to survey seafloor continuously. Since all the data is collected simultaneously and co-located, the output three systems can be cross-referenced without localization errors and compared easily, which is very useful for Mn-crust volumetric estimation purposes.

A. Multibeam sonar

The authors used an Imagenex Model 837B "Delta T" multibeam profiling sonar for wide area acoustic observation of the seafloor. Delta-T is an underwater imaging sonar with 120 beams resolved digitally. It is controlled from a dedicated beamforming software running over an ethernet link. The detailed specifications of the sonar are given in Table I. The data is recorded using the Delta-T software in the 837 format which contains reflection information for all range bins of each of the beams. This data is post-processed to generate bathymetry and intensity maps of the seafloor.

B. Visual mapping system

The visual mapping system is based on the light-sectioning based seafloor 3D mapping system developed in [19]. It consists of a sheet laser, LEDs for illumination, and a camera which records the laser projection on the seafloor and generate

visual color reconstructions of the seafloor. Although the swath of this system is narrower than the multibeam sonar, the resolution is significantly higher at ∼1.4 mm. Since this system generates both bathymetry and colourmaps of the seafloor, it can be used as ground truth for recognizing Mn-crusts [12], and for referencing the multibeam data.

C. Acoustic sub-bottom probe

The acoustic probe is a parametric subsurface sonar that records subsurface reflections of the seafloor for estimating the Mn-crust thickness. The probe consists of a five-channel annular array of 2-MHz piezoelectric transducers for transmission and a 200-kHz piezoelectric transducer to record reflections. It is dynamically focused on the seafloor at ranges from 0.5 to 2.5 m. Details on the system can be found in [11]. The thickness results are not included in this paper.

D. Overall setup

The above systems were attached as payload on the ROV (Perry Slingsby Systems, Ltd.), a photograph of which is shown in Fig. 2. The components were fixed onto a rigid frame which allowed the distance between the multibeam sonar, visual imaging system and the acoustic sub-bottom probe to be kept constant. A Doppler Velocity Log (DVL), depth sensor and interferometric fiber-optic gyroscope based Inertial Measurement Unit (IMU) were also mounted on the same frame for navigational purposes. The absolute location of the ROV was measured from the mother ship using an Ultra Short BaseLine (USBL) system. Combining the USBL data with the dead reckoned position obtained by integrating the depth, IMU measurements and velocity measurements from the frame mounted sensors, an accurate position of the ROV was estimated. Since all components were rigidly attached to the same payload frame, the estimated positional data is used for processing both visual and acoustic data.
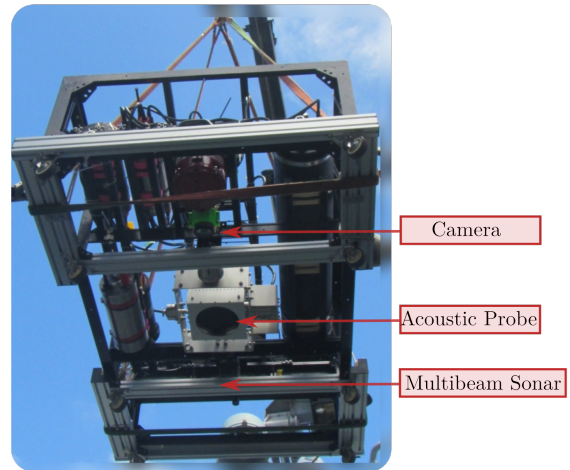

Fig. 2. Photograph of the system mounted on the payload skid of ROV

System	Parameter	Value
Mapping ROV	Altitude	1.5,m
	Velocity	0.1 m/s
Multibeam	Swath	6 m
	Horizontal resolution	50 mm
	Vertical resolution	3 mm
	Forward resolution	6.7 mm
Visual system	Swath	1.5 m
	Horizontal resolution	1.4 mm
	Vertical resolution	3.0 mm
	Forward resolution	6.7 mm

Fig. 3. Visual 3D map and bathymetry for a pillowy Mn-crust area with sediment cover

III. FIELD SURVEYS AND DATA PROCESSING

A. Survey

The above system was deployed in field experiments conducted at a Mn-crust covered seamount at depths ranging between 1350 m to 1550 m. The ROV surveyed the seafloor at a velocity of 0.2 kn (0.1 m/s). The target altitude of the survey was set at 1.5 m. The resultant swaths and resolutions obtained from the two systems are shown in Table II. It can be seen that the multibeam sonar covers 4x area as that of the visual subsystem at a significantly reduced lateral (horizontal) resolution.

B. Data processing

1) Multibeam sonar: The Delta-T multibeam ping data is recorded in 837 format containing the reflection information for all 5000 bins of each of the 120 beams. The seafloor is identified in each of the 120 beams as the bin with the strongest reflection and exported into a single file containing information for all the pings. For each ping, the bin locations for 120 beams and their corresponding intensities are extracted from this file along with the time when the ping was recorded. Using the beam geometry and the range resolution set during recording, the bin locations are converted into robot frame coordinates. The position and orientation of the vehicle at the time when the ping was recorded is then used to convert the detected seafloor point cloud into earth frame coordinates.

The reflection intensity values are strongly affected by the beam geometry with the central beams having a stronger value. To compensate for this, the angular response of the sonar is estimated by taking an average of the intensity values for each beam across all the pings where the seafloor has been detected. This angular response is then used to compensate for the beam geometry while calculating the reflection intensity value for the detected seafloor bins.

2) Visual mapping: The images with laser line projections are recorded during the survey. The laser line is detected in the images and converted into robot frame coordinates considering the geometry of the system. The position and orientation of the vehicle is then used to convert the point cloud into earth coordinates. Color information is also obtained for the points identified by the laser generating a visual color reconstruction of the seafloor in 3D.
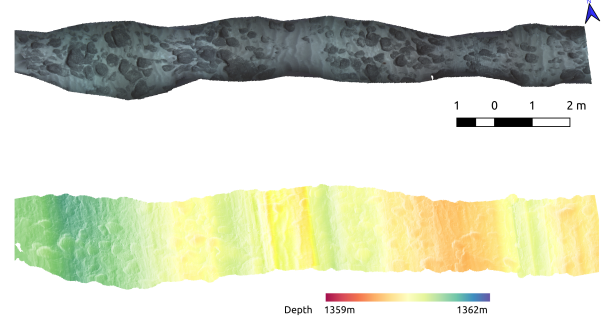
C. Initial results

Data was collected over varying terrains consisting of Mn-crusts, sediment patches and Mn-nodules. Patches of different terrain were used for used for analyzing the multibeam data and comparing it with the visual mapped data. Three example sections showing different landscapes are shown below.

1) Pillowy Mn-crust with sediment cover: Figures 3 and 4 show an area with pillowy Mn-crust covered with sediment. The top view of the color 3D reconstruction, hillshaded bathymetric map, backscatter map generated by the multibeam sonar and the bathymetric map generated by the multibeam sonar are shown respectively. The texture of the seafloor is clearly visible in visual and backscatter maps. Artifacts due to the irregular motion of the ROV is visible in the visual bathymetry maps.
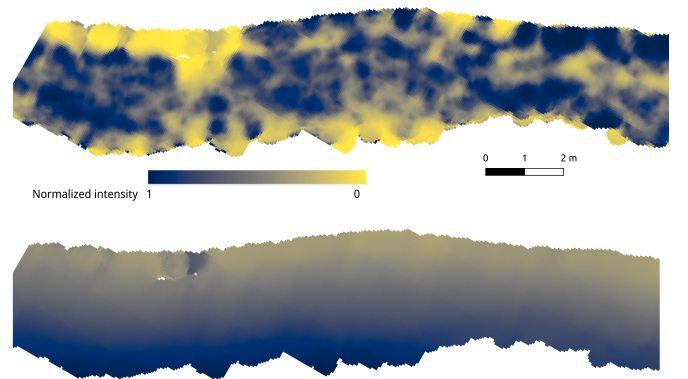

Fig. 4. Multibeam backscatter and bathymetry for the area shown in Fig. 3

2) Mixed area: Fig. 5 shows an area with varying seafloor for highlighting the advantage of multibeam surveys. Fig. 5a

shows the normalized backscatter intensity and Fig. 5b shows the corresponding 3D color reconstruction of the seafloor. Sediment deposits can be seen towards the left and the lower middle sections of the graph. The other sections contains rocky Mn-crusts of various sizes. The difference in the swath shows clearly the variation of the Mn-crust distribution. Although the visual map indicates three sediment covered sections, the third section appears to be very small as seen in the backscatter map. Artifacts due to saturation of the central beams of the sonar are also visible in the sediment areas. It can also be seen that the backscatter intensity shows variations similar to that of the luminous intensity of the visual 3D map.

IV. Visual seafloor classification

Being able to distinguish Mn-crust deposits from sediments in Fig. 5, the possibility of automatic classification of the multibeam data for seafloor characterization is investigated below. The authors have developed a machine learning based method for identifying Mn-crust from seafloor bathymetry and color maps [20]. The seafloor is divided into uniform sized kernels and parameters denoting the color, texture, bathymetry, and roughness are extracted for each kernel. The kernels are then classified into either Mn-crust, Mn-nodules, or sediments based on this parameter vector using an SVM classifier with a polynomial kernel. The choice of parameters and the effect on the classification performance was investigated in detail [12].

Transfer learning is the method of utilizing the knowledge gained in one domain in another familiar domain, by exploiting the similarity in data [21]. This is beneficial in developing machine learning classifiers where labelled training data is limited or unavailable. In the case of multibeam characterization, the similarity of the backscatter intensity to the luminous intensity of the visual 3D map is utilized. Since bathymetric information is available from both sources, albeit at different resolutions, it is also incorporated.

An SVM classifier was developed using expert labelled seafloor 3D visual mapping data, classified into Mn-crusts, sediments or Mn-nodules. For a kernel size of 30 cm, a total of 11 parameters are calculated representing the texture, luminosity, roughness and slope. All parameters were normalized to zero mean and unit standard deviation. An SVM classifier is trained using the training data, with an accuracy of 90%, measured on a separate testing dataset also generated from the visual 3D data.

This classifier was then used to classify the multibeam generated data, by replacing the luminosity of the visual 3D maps with the backscatter intensity of the multibeam. The parameters were calculated using the same kernel size of 30 cm. The density of points is, however, low due to the lower resolution of the multibeam. Preliminary results from classification is shown in Fig. 6. For seafloor section from Fig. 5, the multibeam backscatter intensity and the classification results are shown.

The results are promising, but require further tuning. Calculation of the accuracy of classification and confusion matrices by referencing them to co-located visual 3D maps is necessary.

Further tuning the transfer learned classifier using co-located data is not possible using an SVM classifier, but can be done using deep learning methods in conjunction.

V. Conclusion

This paper presents the preliminary results from surveying deep sea Mn-crust deposits using a multibeam sonar together with a 3D mapping system. Data from selected regions are presented and the results from the two systems were compared. Further, using transfer learning, a machine learning classifier trained on visual data is used to classify the multibeam generated data, with promising results. This is useful to compensate for the lack of ground truth data for the multibeam systems. The results can be further improved by tuning the parameters and using alternate classifier methodologies. The co-located data from these sources can be used to extend the area coverage of visual 3D mapping systems and provide larger area Mn-crust volumetric estimates.

References

[1] J. R. Hein, K. Mizell, A. Koschinsky, and T. A. Conrad, "Deep-ocean mineral deposits as a source of critical metals for high- and green-technology applications: Comparison with land-based resources," *Ore Geology Reviews*, vol. 51, pp. 1–14, Jun. 2013, publisher: Elsevier B.V. ISBN: 0169-1368.

[2] M. R. Clark, R. Heydon, J. R. Hein, S. Petersen, A. Rowden, S. Smith, E. Baker, and Y. Beaudoin, *Deep Sea Minerals: Cobalt-rich Ferromanganese Crusts, a physical, biological, environmental, and technical review*, E. Baker and Y. Beaudoin, Eds. Secretariat of the Pacific Community, 2013, publication Title: Deep Sea Minerals.

[3] P. A. J. Lusty and B. J. Murton, "Deep-Ocean Mineral Deposits: Metal Resources and Windows into Earth Processes," *Elements*, vol. 14, no. 5, pp. 301–306, Oct. 2018.

[4] P. A. J. Lusty, J. R. Hein, and P. Josso, "Formation and Occurrence of Ferromanganese Crusts: Earth's Storehouse for Critical Metals," *Elements*, vol. 14, no. 5, pp. 313–318, Oct. 2018.

[5] A. Usui, K. Nishi, H. Sato, Y. Nakasato, B. Thornton, T. Kashiwabara, A. Tokumaru, A. Sakaguchi, K. Yamaoka, S. Kato, S. Nitahara, K. Suzuki, K. Iijima, and T. Urabe, "Continuous growth of hydrogenetic ferromanganese crusts since 17 Myr ago on Takuyo-Daigo Seamount, NW Pacific, at water depths of 800–5500 m," *Ore Geology Reviews*, vol. 87, pp. 71–87, Jul. 2017, publisher: Elsevier B.V.

[6] International Seabed Authority, "Regulations on Prospecting and Exploration for Cobalt-rich Ferromanganese Crusts in the Area," 2012, issue: October.

[7] J. Joo, S. S. Kim, J. W. Choi, S. J. Pak, Y. Ko, S. K. Son, J. W. Moon, and J. Kim, "Seabed mapping using shipboard multibeam acoustic data for assessing the spatial distribution of ferromanganese crusts on seamounts in the western pacific," *Minerals*, vol. 10, no. 2, pp. 1–20, 2020.

[8] B. Zhao, Y. Yang, X. Zhang, G. He, W. Lü, Y. Liu, Z. Wei, Y. Deng, and N. Huang, "Sedimentary characteristics based on sub-bottom profiling and the implications for mineralization of cobalt-rich ferromanganese crusts at Weijia Guyot, Western Pacific Ocean," *Deep Sea Research Part I: Oceanographic Research Papers*, vol. 158, p. 103223, Apr. 2020.

[9] D. Du, X. Ren, S. Yan, X. Shi, Y. Liu, and G. He, "An integrated method for the quantitative evaluation of mineral resources of cobalt-rich crusts on seamounts," *Ore Geology Reviews*, vol. 84, pp. 174–184, 2017, publisher: Elsevier B.V.
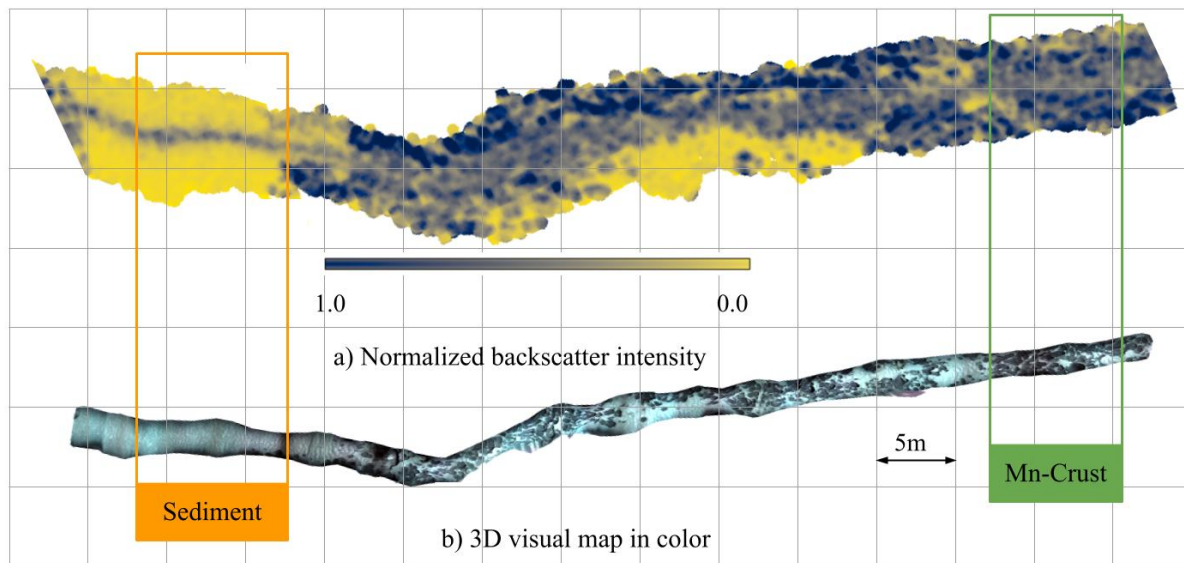
Fig. 5. Multibeam backscatter and bathymetry for a seafloor section containing rocky Mn-crusts, pillowy Mn-crusts and sediment deposits
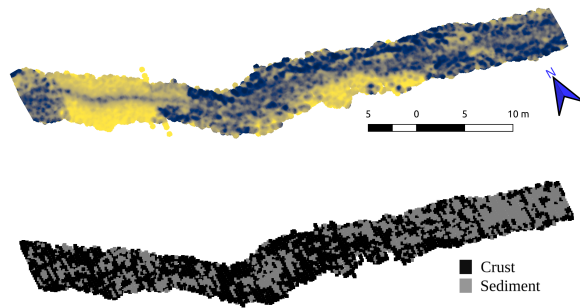

Fig. 6. Preliminary results from classification of multibeam data with an SVM classifier. The classifier was trained on the 3D mapping data, but tested using the multibeam data.

[10] D. Du, C. Wang, X. Du, S. Yan, X. Ren, X. Shi, and J. R. Hein, "Distance-gradient-based variogram and Kriging to evaluate cobalt-rich crust deposits on seamounts," *Ore Geology Reviews*, vol. 84, pp. 218–227, 2017, publisher: Elsevier B.V.

[11] B. Thornton, A. Asada, A. Bodenmann, M. Sangekar, and T. Ura, "Instruments and methods for acoustic and visual survey of manganese crusts," *IEEE Journal of Oceanic Engineering*, vol. 38, no. 1, pp. 186–203, Jan. 2013, iSBN: 0364-9059 VO - 38.

[12] U. Neettiyath, B. Thornton, M. Sangekar, Y. Nishida, K. Ishii, A. Bodenmann, T. Sato, T. Ura, and A. Asada, "Deep-Sea Robotic Survey and Data Processing Methods for Regional-Scale Estimation of Manganese Crust Distribution," *IEEE Journal of Oceanic Engineering*, vol. 46, no. 1, pp. 102–114, Jan. 2021.

[13] R. Michaelis, H. C. Hass, and S. Papenmeier, "Automated Stone Detection on Side-Scan Sonar Mosaics Using Haar-Like Features," *Geosciences*, 2019.

[14] A. G. P. V. Dijk and D. G. Simons, "Geostatistical modelling of multibeam backscatter for full- coverage seabed sediment maps," *Hydrobiologia*, vol. 4, pp. 55–79, 2019, iSBN: 0123456789.

[15] E. Alevizos, T. Schoening, K. Koeser, M. Snellen, and J. Greinert, "Quantification of the fine-scale distribution of Mn-nodules: insights from AUV multi-beam and optical imagery data fusion," *Biogeosciences Discussions*, no. February, pp. 1–29, 2018.

[16] I. Z. Gazis, T. Schoening, E. Alevizos, and J. Greinert, "Quantitative mapping and predictive modeling of Mn nodules' distribution from hydroacoustic and optical AUV data linked by random forests machine learning," *Biogeosciences*, vol. 15, no. 23, pp. 7347–7377, 2018.

[17] L. J. Wong, V. Pallayil, M. P, A. K, B. Kalyan, V. N. Hari, M A Atmanand, and M. Chitre, "Acoustic Backscattering Properties of Polymetallic Nodules from the Indian Ocean Basin : Results from a Laboratory Measurement," in *UT Kaohsiung*, 2019.

[18] L. J. Wong, B. Kalyan, M. Chitre, and H. Vishnu, "Acoustic Assessment of Polymetallic Nodule Abundance Using Sidescan Sonar and Altimeter," *IEEE Journal of Oceanic Engineering*, vol. 46, no. 1, pp. 132–142, 2020, publisher: IEEE.

[19] A. Bodenmann, B. Thornton, and T. Ura, "Generation of High-resolution Three-dimensional Reconstructions of the Seafloor in Color using a Single Camera and Structured Light," *Journal of Field Robotics*, vol. 34, no. 5, pp. 833–851, Dec. 2017, arXiv: 10.1.1.91.5767 ISBN: 9783902661623.

[20] U. Neettiyath, T. Sato, M. Sangekar, A. Bodenmann, B. Thornton, T. Ura, and A. Asada, "Identification of manganese crusts in 3D visual reconstructions to filter geo-registered acoustic sub-surface measurements," in *OCEANS 2015 - MTS/IEEE Washington*. IEEE, Oct. 2015, pp. 1–6.

[21] A. Jain, S. Srivastava, and S. Soman, "Transfer learning using adaptive SVM for image classification," in *2013 IEEE Second International Conference on Image Information Processing (ICIIP-2013)*. Shimla, India: IEEE, Dec. 2013, pp. 580–585.